# Black Phosphorus-Graphite Material Composites with a Low Activation Energy of Interfacial Conductivity

AUTHOR(S):

JU, Yuhang; NASARA, Ralph Nicolai; LEE, Changhee; MIYAHARA, Yuto; ABE, Takeshi; MIYAZAKI, Kohei

CITATION:

JU, Yuhang ...[et al]. Black Phosphorus-Graphite Material Composites with a Low Activation Energy of Interfacial Conductivity. Electrochemistry 2022, 90(2): 027007.

ISSUE DATE:

2022-02

URL:

http://hdl.handle.net/2433/277041

Electrochemistry
The Electrochemical Society of Japan
Received: December 25, 2021
Accepted: January 14, 2022
Published online: January 19, 2022
Issued: February 17, 2022
J-STAGE https://doi.org/10.5796/electrochemistry.21-00132
Article Electrochemistry, 90(2), 027007 (2022)

# Black Phosphorus-Graphite Material Composites with a Low Activation Energy of Interfacial Conductivity

OPEN ACCESS

Yuhang JU, Ralph Nicolai NASARA, Changhee LEE,§ Yuto MIYAHARA,§ Takeshi ABE,§ and Kohei MIYAZAKI*,§

*Graduate School of Engineering, Kyoto University, Nishikyo-ku, Kyoto 615-8510, Japan*

* *Corresponding author: myzkohei@elech.kuic.kyoto-u.ac.jp*

**ABSTRACT**

The reaction kinetics of electrochemical lithiation/delithiation in a composite consisting of black phosphorus and cup-stacked carbon nanotube (BP-CSCNT) were investigated. Two semicircles were observed in Nyquist plots at the high and low frequency regions, which were attributed to the resistance of lithium-ion transport through the surface film and the resistance of the alloying/dealloying reaction (charge-transfer resistance), respectively. The activation energy using the charge transfer reaction was evaluated from the temperature-dependence of the interfacial conductivity. Even with the use of ethylene carbonate-based and propylene carbonate electrolytes, the activation energy was calculated to be 25–26 kJ mol$^{-1}$, which is much smaller than that obtained with graphite electrodes and cathode materials. These results indicate that the ionic charge transfer process in BP-CSCNT composite electrodes is not coupled with the desolvation process and suggest that the charge transfer in BP-CSCNT is exceptionally fast compared to that in other insertion materials.



Keywords : Black Phosphorus, Activation Energy, Lithium Charge Transfer, Solvent De-solvation Process

## 1. Introduction

Rechargeable lithium-ion batteries (LIBs) are widely used as a key power source for portable electric devices, electric vehicles (EVs), and large-scale stationary energy storage systems (ESS). However, several optimizations are needed to further promote the application of LIBs, especially for use in EVs and ESSs. To date, graphite which has a theoretical capacity of 372 mAh g$^{-1}$, has been widely used as a negative electrode material for LIBs, but alternative materials with higher capacity are being actively pursued. For example, alloying-type materials such as phosphorus (P) and silicon (Si) have attracted attention as new negative materials.[1,2] These materials electrochemically react with lithium ions to form lithium alloys that can deliver an extremely high energy density compared to graphite. Among the alloy-based anode materials, black phosphorus (BP) has several attractive properties such as a high-rate capability and large capacity in lithium storage (theoretical capacity of 2596 mAh g$^{-1}$).[3] Furthermore, the relatively high electric conductivity of BP (~300 S m$^{-1}$) is another reason why it should be considered for LIB applications.[4]

Generally, the capacity of alloy-based anode materials deteriorates rapidly due to the change in the volume of active materials caused by the insertion and deinsertion of lithium ions.[1,5] In the case of BPs, composition with germanium (Ge) or graphite has been widely studied and is known to be very effective in improving cycle performance.[6–11] However, the details of the kinetics of the lithium-ion transfer reaction at the active material interface that is newly formed by composition are still unknown. The kinetics at the active material interface is a very important factor in defining the electrode performance, especially since the current per C-rate is large for large-capacity anodes.

We have previously studied the kinetic properties of various systems including anode materials, cathode materials, and solid electrolytes, and found that (i) the activation energy of interfacial lithium-transfer reactions is around 50 kJ mol$^{-1}$ or higher, and (ii) the activation energy depends on the type of solvent.[12,13] Since different solvents have different binding forces with lithium ions, ion transfer from electrolyte to electrode shows different desolvation energies in various electrolytes. To the best of our knowledge, no previous studies have clarified the kinetic properties of BP-based materials electrodes by describing the interfacial ion-transfer reaction.

In this study, we used AC impedance spectroscopy to study the kinetics of the charge transfer reaction for a hybrid material of BP and cup-stack carbon nanotube (CSCNT). CSCNT is a nanotube material with many exposed graphite edge surfaces,[14,15] which are highly reactive and suitable for effective composition with BP.

## 2. Experimental

BP powder and CSCNT were supplied by Rasa Industries Ltd. and GSI Creos Corporation, respectively. Composites of BP and CSCNT (mixed ratio of 1 : 1 by weight) were prepared by mechanical ball-milling (PL-7, Fritsch) using $ZrO_2$ balls (5 mm) in a 50 mL $ZrO_2$ pot with a ball-to-powder mass ratio of 40 : 1. The rotation speed was 450 rpm, and ball-milling was carried out under an Ar atmosphere (solvent-free) for 12 h. After the initial ball-milling was completed, acetylene black (AB, HS-100, Denka) as a conductive additive was subsequently added and mixed with BP-CSCNT (150 rpm, BP-CSCNT : AB = 8 : 1 by weight). After blending with a binder in *N*-methyl-2-pyrrolidone solutions, a slurry containing a mixture of BP-CSCNT powder (80 wt%), AB (10 wt%), and binder (10 wt%) was coated on a copper foil in a glove box ($H_2O$ < 1 ppm, $O_2$ < 1 ppm). After being dried under vacuum for 12 h, the slurry was pressed at 10 MPa for 4 s to enhance the contact between BP and CSCNT. The morphology of the BP-CSCNT powder was observed by transmission electron microscopy (TEM) measurements using a Hitachi TEM H-9000 type NAR.

§ECSJ Active Member
R. N. Nasara orcid.org/0000-0003-4853-7387
Y. Miyahara orcid.org/0000-0003-4662-0996
K. Miyazaki orcid.org/0000-0001-5177-3570
T. Abe orcid.org/0000-0002-1515-8340

The electrolyte solutions used were 1 mol dm$^{-3}$ (M) $LiClO_4$ dissolved in propylene carbonate (PC), a mixture of ethylene carbonate (EC) and diethyl carbonate (DEC) (EC+DEC, 1 : 1 by volume), and a mixture of fluoroethylene carbonate (FEC) and dimethyl carbonate (DMC) (FEC+DMC, 3 : 7 by volume) (all of these chemicals were purchased from Tomiyama Chemical Co. Ltd.). Electrochemical measurements were carried out using 2032-type coin cells (BP-CSCNT/Li metal) and three-electrode cells. Cyclic voltammetry (CV) at a scan rate of 1 mV s$^{-1}$ and constant current charge/discharge tests (0.1 C rate) were performed in a potential range of 0.001–2.5 V. A Solartron 1480 Multistat (Solartron Analytical) and an SI 1255 frequency response analyzer were used for electrochemical measurements. After 3 cycles of CV, electrochemical impedance spectroscopy (EIS) was performed over a frequency region of 100 kHz to 10 mHz with an amplitude of 5 mV. All charge/discharge capacity calculations were based on the total weight of BP and CSCNT used as the active material (1800 mAh g$^{-1}$).

## 3. Results and Discussion

A TEM image of a BP-CSCNT composite powder is shown in Fig. 1A. The structure of the BP particles was found to be covered and wrapped by an amorphous layer of carbon material. It is thought that the energy of mechanical ball-milling destroyed the cup-stack structure of the CSCNT and formed a bond between C and P, resulting in the ball-like shape. Based on this TEM image, Fig. 1B offers a possible schematic of BP covered with amorphous carbon material.

The results of constant-current charge-discharge measurements and d$Q$/d$V$ curves are shown in Fig. 2. Although there was an irreversible capacity of about 370 mAh g$^{-1}$ in the first cycle, the discharge capacity was stable for up to three cycles at a value of 1250 mAh g$^{-1}$. This discharge capacity is comparable to that of the BP composite reported so far,[11] indicating that it is possible to obtain a high-capacity anode with excellent stability by using CSCNT as a carbon material. The CVs measured with FEC+DMC (3 : 7 by volume) and PC as electrolytes are shown in Fig. 3. As a result, the peak current values of oxidation and reduction gradually decreased with CV cycling. Thereafter, we proceeded with the experiment using EC+DEC as the electrolyte, which had the highest stability.

To investigate the lithium-ion transfer reaction of BP-CSCNT in detail, electrochemical impedance measurements were carried out using a three-electrode cell. Figure 4A shows Nyquist plots measured after three cycles of CV to form an SEI film on the surface of BP-CSCNT electrodes. The Nyquist plot at OCV (2.5 V) shows one semicircle with a characteristic frequency of 3160 Hz. When the electrode potential decreased below 1.0 V, another semicircle appeared with a characteristic frequency of 30–80 Hz. Since a three-electrode system was used in this measurement, the resistance from the lithium metal (counter electrode, CE) can be ignored. Therefore, we can focus on charge-transfer resistances ($R_{ct}$) and lithium-ion transport resistances within SEI films ($R_{SEI}$) in this system. The intercept component of the $Z'$ axis seen in the plot with the highest frequency is the sum of the resistances associated with electron conduction ($R_e$) and solution resistance ($R_s$). The lithium diffusion resistance in the electrode is also excluded from the

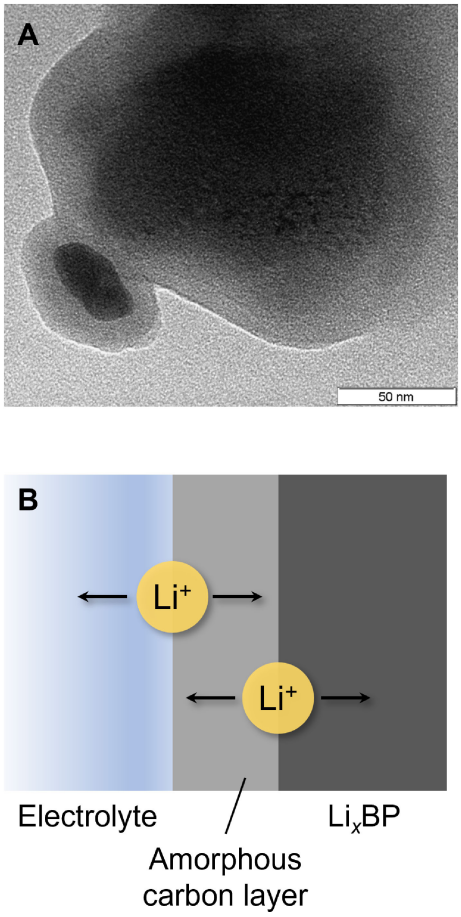


**Figure 1.** (A) TEM image of a BP-CSCNT particle and (B) proposed schematic diagram of possible electrochemical processes at BP-CSCNT composite electrodes.

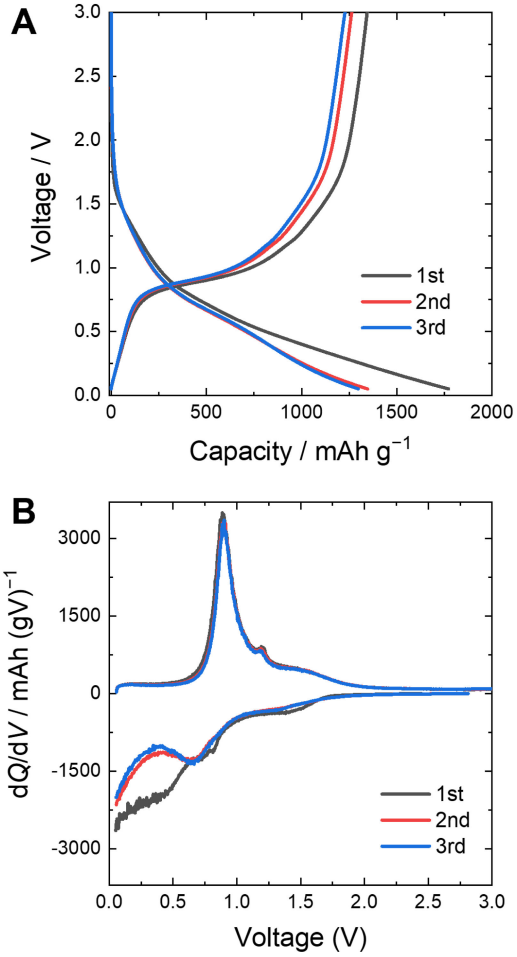


**Figure 2.** (A) Charge-discharge curves and (B) d$Q$/d$V$ curves for a BP-CSCNT electrode in 1 mol dm$^{-3}$ $LiClO_4$/EC+DEC (1 : 1 by volume).

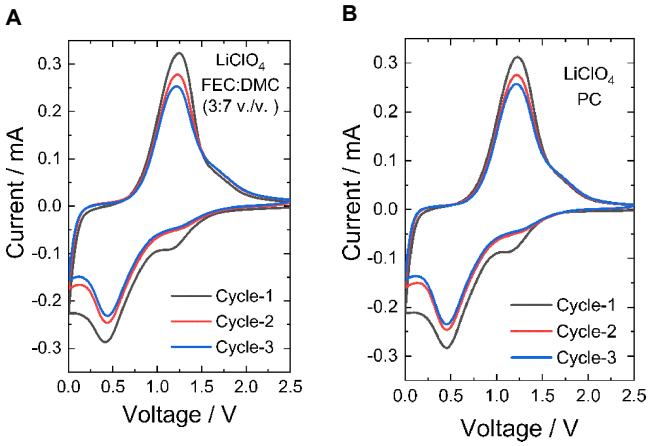


**Figure 3.** Cyclic voltammograms of a BP-CSCNT electrode in (A) 1 mol dm$^{-3}$ $LiClO_4$/FEC+DMC (3 : 7 by volume) and (B) 1 mol dm$^{-3}$ $LiClO_4$/PC.

charge-transfer resistances because the impedance has an almost 45° tail in the low frequency region.

The equivalent circuit shown in the inset of Fig. 4A was used to fit the electrochemical impedance measurement results. This equivalent circuit consists of one resistive component ($R_e + R_s$), two RC parallel elements ($R_{ct}$//CPE and $R_{SEI}$//CPE), and one Warburg impedance. Figure 4B shows changes in Nyquist plots in a potential range of 0.60–0.20 V. The semicircle with a high characteristic frequency remained at a constant diameter regardless of the potential, while the semicircle with a low characteristic frequency showed a rapid decrease in diameter as the potential dropped below 0.6 V. Of the two RC parallel elements, $R_{ct}$ is the one that exhibits potential responsivity, so the semicircles with a characteristic frequency of 30–80 Hz are attributed to interfacial charge transfer. Based on the attribution of the impedance measurement results, the variation of $R_{ct}$ and $R_{SEI}$ with respect to the potential is shown in Fig. 4C. This Figure also shows that $R_{SEI}$ was constant regardless of the potential, but $R_{ct}$ decreased as the potential decreased.

Next, we discuss the temperature-dependence of the charge-transfer resistance. The interfacial conductivity ($1/R_{ct}$) obeys the Arrhenius equation as follows:

$$\frac{1}{R_{ct}} = A \exp\left(-\frac{E_a}{RT}\right)$$

where $A$, $E_a$, $R$, and $T$ denote the frequency factor, activation energy, gas constant, and absolute temperature, respectively. Previous studies have shown that the activation energy of the interfacial conductivity is closely related to the desolvation energy of lithium ion. In this study, we also investigated the temperature-dependence of the interfacial conductivity using three different solvents.[12,13,16] The interfacial conductivity ($1/R_{ct}$) at 0.7 V for cells with various electrolytes is shown in Fig. 5. Each plot shows good linearity and follows the Arrhenius equation shown above. From the slope of the lines, the activation energy was calculated to be 25–26 kJ mol$^{-1}$. Interestingly, the activation energies with different solvent systems are not very different from each other. Basically, these three solvents have quite different affinities for lithium ions. Among the solvents used here, the magnitude of the solvation ability for each solvent molecule is in the order PC > EC > DMC ≈ FEC.[17–19] In a previous study using $Li_4Ti_5O_{12}$, the activation energies were in the order PC (64–66 kJ mol$^{-1}$) > EC+DEC (1 : 1) (52–56 kJ mol$^{-1}$) > FEC+DMC (3 : 7) (33–36 kJ mol$^{-1}$), which is in good agreement with the solvation capacity of the solvent molecules.[20] However, our

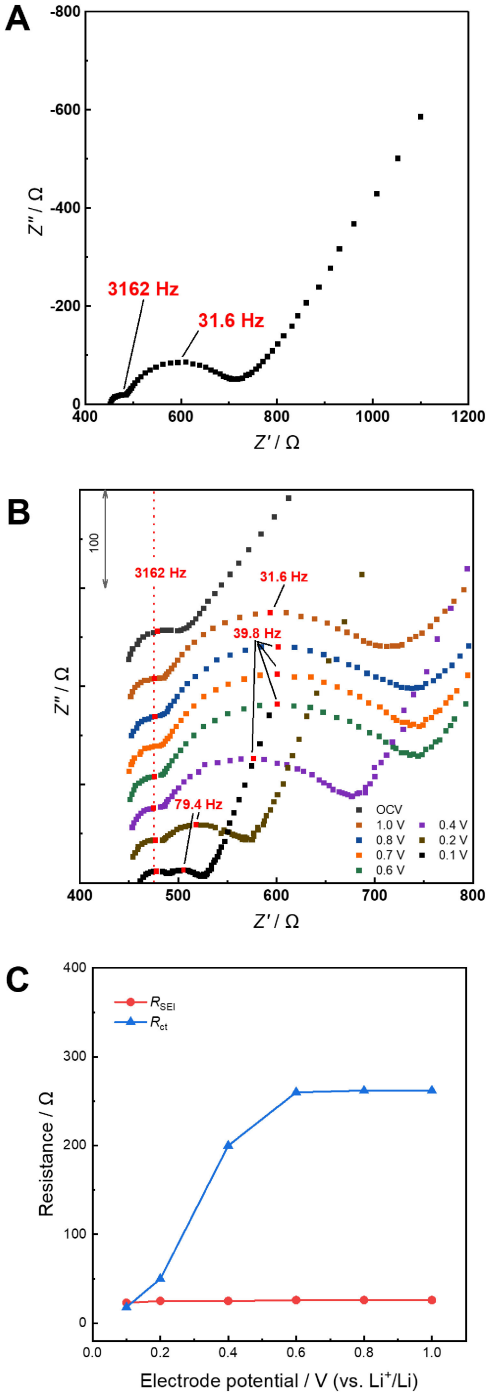


**Figure 4.** (A) Nyquist plot for a BP-CSCNT composite electrode after 3 cycles at 0.4 V using an EC+DEC solution. (B) Nyquist plots of BP-CSCNT in 1 mol dm$^{-3}$ $LiClO_4$/EC+DEC at various potentials after 3 cycles. (C) Potential dependence of the charge-transfer resistance ($R_{ct}$) and the ion-transport resistance in the SEI ($R_{SEI}$). All experiments were performed at 30 °C.

BP-CSCNT show the same activation energies in all three solvents, suggesting that they are less related to the desolvation process.

We can offer two possible reasons why the activation energy of interfacial conductivity was not solvent-dependent. The first possibility is that the active material BP is covered with an amorphous layer of carbon, as shown in the TEM image, and this prevents the activation energy from being explained by simple desolvation. The solvated lithium ions are desolvated stepwise inside the amorphous layer of carbon, leading to a lower activation

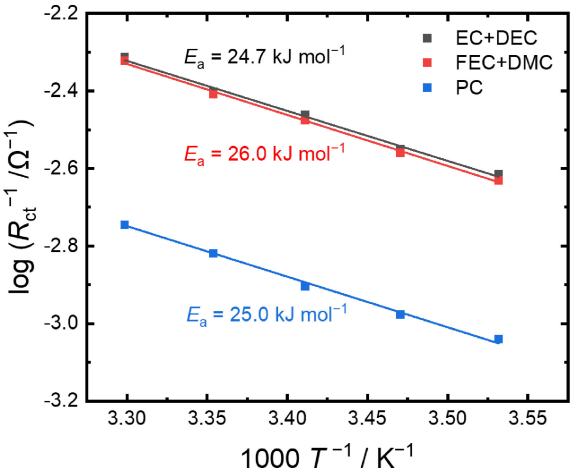


**Figure 5.** Temperature dependence of interfacial conductivities ($1/R_{ct}$) on BP-CSCNT in various electrolytes. The interfacial conductivities were obtained from Nyquist plots at 0.7 V in a temperature range of 10–30 °C.

barrier. For example, it is known that the activation energy changes depending on the presence and type of SEI, and a similar phenomenon may have occurred.[21,22] The second possibility is that the activation energy is different between the active material of the insertion system and the active material of the alloy/de-alloy system. Electrochemical impedance results for SiO (Si/$SiO_2$), one of the alloy anodes, also showed activation energies of 29–32 kJ mol$^{-1}$ in various solvents.[17] The reason for the very low activation energies of the alloy-based active materials is still unclear but may be related to intrinsic differences in the electrode reactions. A more detailed analysis is needed to clarify which hypothesis is correct.

As shown above, BP-CSCNT, which is a composite of BP and CSCNT, is very attractive as an anode material because of its low irreversible capacity during charging and discharging, high capacity, and low activation energy of interfacial conductivity. It is expected that higher-performance anodes may be constructed following further studies on structural analysis, rate characteristics, and optimization of the composite, etc.

## 4. Conclusions

A composite of black phosphorus and graphite material was examined, and the results showed that the activation energy of lithium-ion transfer at the interface is smaller than those for other insertion electrodes such as graphite and cathode materials. Therefore, the BP composite has a kinetic advantage over other insertion materials. Furthermore, the activation energy of charge transfer at the BP composite electrode did not change among different electrolytes. These results suggest that the rate of charge transfer in BP composites is not affected by the desolvation of lithium ions, which is the rate-limiting step of charge transfer for other conventional insertion electrodes.

## CRediT Authorship Contribution Statement

Yuhang Ju: Data curation (Equal), Writing – original draft (Equal)
Ralph Nicolai Nasara: Data curation (Equal)
Changhee Lee: Project administration (Equal)
Yuto Miyahara: Project administration (Equal)
Takeshi Abe: Supervision (Equal)
Kohei Miyazaki: Supervision (Equal), Writing – review & editing (Equal)

## Conflict of Interest

The authors declare no conflict of interest in the manuscript.

## References

1. M. N. Obrovac and V. L. Chevrier, *Chem. Rev.*, **114**, 11444 (2014).
2. Y. Fu, Q. Wei, G. Zhang, and S. Sun, *Adv. Energy Mater.*, **8**, 1703058 (2018).
3. M. Qiu, Z. T. Sun, D. K. Sang, X. G. Han, H. Zhang, and C. M. Niu, *Nanoscale*, **9**, 13384 (2017).
4. R. W. Keyes, *Phys. Rev.*, **92**, 580 (1953).
5. C.-M. Park, J.-H. Kim, H. Kim, and H.-J. Sohn, *Chem. Soc. Rev.*, **39**, 3115 (2010).
6. X. Li, W. Li, P. Shen, L. Yang, Y. Li, Z. Shi, and H. Zhang, *Ceram. Int.*, **45**, 15711 (2019).
7. W. Li, H. Li, Z. Lu, L. Gan, L. Ke, T. Zhai, and H. Zhou, *Energy Environ. Sci.*, **8**, 3629 (2015).
8. K.-W. Tseng, S.-B. Huang, W.-C. Chang, and H.-Y. Tuan, *Chem. Mater.*, **30**, 4440 (2018).
9. H. Shin, J. Zhang, and W. Lu, *Electrochim. Acta*, **309**, 264 (2019).
10. S. Haghighat-Shishavan, M. Nazarian-Samani, M. Nazarian-Samani, H.-K. Roh, K.-Y. Chung, B.-W. Cho, S. F. Kashani-Bozorg, and K.-B. Kim, *J. Mater. Chem. A*, **6**, 10121 (2018).
11. H. Jin, S. Xin, C. Chuang, W. Li, H. Wang, J. Zhu, H. Xie, T. Zhang, Y. Wan, Z. Qi, W. Yan, Y.-R. Lu, T.-S. Chan, X. Wu, J. B. Goodenough, H. Ji, and X. Duan, *Science*, **370**, 192 (2020).
12. Z. Ogumi, *Electrochemistry*, **78**, 319 (2010).
13. T. Abe, H. Fukuda, Y. Iriyama, and Z. Ogumi, *J. Electrochem. Soc.*, **151**, A1120 (2004).
14. Y. Iwahori, S. Ishiwata, T. Sumizawa, and T. Ishikawa, *Compos. Part Appl. Sci. Manuf.*, **36**, 1430 (2005).
15. T. Yokozeki, Y. Iwahori, and S. Ishiwata, *Compos. Part Appl. Sci. Manuf.*, **38**, 917 (2007).
16. K. Xu and A. von Wald Cresce, *J. Mater. Res.*, **27**, 2327 (2012).
17. Y. Yamada, Y. Iriyama, T. Abe, and Z. Ogumi, *J. Electrochem. Soc.*, **157**, A26 (2010).
18. C.-C. Su, M. He, R. Amine, T. Rojas, L. Cheng, A. T. Ngo, and K. Amine, *Energy Environ. Sci.*, **12**, 1249 (2019).
19. X. Liu, J. Zhou, Z. Xu, and Y. Wang, *RSC Adv.*, **10**, 16302 (2020).
20. R. N. Nasara, W. Ma, Y. Kondo, K. Miyazaki, Y. Miyahara, T. Fukutsuka, C. Lin, S. Lin, and T. Abe, *ChemSusChem*, **13**, 4041 (2020).
21. Y. Yamada, Y. Iriyama, T. Abe, and Z. Ogumi, *Langmuir*, **25**, 12766 (2009).
22. K. Xu, A. von Cresce, and U. Lee, *Langmuir*, **26**, 11538 (2010).